

Electrocatalytic oxidation of CO on Ru(0001) surfaces: The influence of surface disorder

J. Lee, W. B. Wang, M. S. Zei* and G. Ertl

Fritz-Haber-Institut der Max-Planck-Gesellschaft, Faradayweg 4–6, D-14195 Berlin, Germany.

E-mail: zei@fhi-berlin.mpg.de

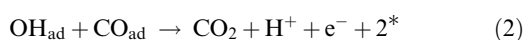
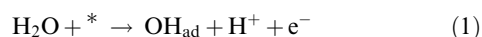
Received 19th October 2001, Accepted 18th February 2002

First published as an Advance Article on the web 12th March 2002

Smooth and rough (created by argon ion sputtering) Ru(0001) surfaces were structurally characterized by reflection high energy electron diffraction (RHEED), and their activity in electrooxidation of CO in 0.1 M HClO₄ solution was probed by cyclic voltammetry (CV). While the peak potentials of CO-oxidation on the smooth surface varied with the CO,OH-adsorbate composition (which changed in subsequent scans), these were markedly (~0.3 V) lower with the rough surface. This difference is attributed to the varying properties of the Ru–O bond whose activation is considered to be rate-limiting. The enhanced activity of the rough surface is also reflected by the fact that the entire amount of adsorbed CO becomes completely oxidized during the first anodic scan, while with the flat surface at least three cycles are required.

1. Introduction

Ru is commonly used to promote CO electrooxidation on Pt in methanol fuel cells,^{1–4} and this effect is essentially attributed to a bifunctional mechanism whereafter Ru adsorbs oxygen-containing species at lower potential than Pt. The electrocatalytic oxidation of CO is believed to proceed along the following mechanism (* denotes the empty site):



On Pt, step (1) is considered to be rate-determining, *i.e.* CO₂ evolution starts as soon as OH_{ad} formation sets in. The situation with pure Ru, however, is different: Adsorption of O-containing species occurs at potentials far below those for CO₂ evolution (and at overpotentials about 300 mV lower than with Pt,^{5,6} so that now step (2) is rate-limiting, – obviously because of the need to activate the stronger M–O bond. Since the properties of the latter are affected by the surface structure of the catalyst we investigated the difference in reactivity between a smooth and a rough Ru(0001) surface in order to get closer insight into the mechanism of the reaction.

2. Experimental

The experiments were performed with an apparatus consisting of a UHV chamber (base pressure < 1.5 × 10^{–10} mbar) incorporating LEED, RHEED and AES, an electrochemical chamber (base pressure < 1.0 × 10^{–9} mbar), an electrochemical cell and a closed sample transfer. The electrochemical cell consists of two parts, and a flow-cell procedure has been used which allows us to change electrolyte solutions under potential control and in an air-free atmosphere.

RHEED was performed with an incident electron beam (40 keV) at a grazing angle of 1–2° to the surface. The RHEED electron beam also acts as the primary electron source for AES. This combination allows RHEED and AES data to be recorded from the same surface region, thus correlating the structure and chemical composition data.

The working electrode, a Ru(0001) single crystal disc of 7 mm diameter and 2 mm thickness, was mounted between tungsten wires which also served for resistive heating of the sample. The electrode surface was prepared by cycles of argon ion bombardments (5 × 10^{–5} mbar, at room temperature and 700 °C), until the sample surface was free from disorder and impurities as controlled by LEED/RHEED and AES. The sample was then transferred to the electrochemical chamber under UHV conditions where the reactivity was probed by cyclic voltammetry (CV). Standard electrochemical equipment was employed for potential sweeping. The electrode surface after the electrochemical treatments and emersion was again characterized by LEED/RHEED and AES. The experimental details have been reported elsewhere.^{7,8}

A platinum wire with 0.4 mm diameter was used as counter electrode in the electrolyte vessel on top of a glass capillary.⁷ CO electrosorption was achieved by immersion of the Ru(0001) electrode in a CO-saturated 0.1 M HClO₄ solution at a potential of –0.1 V for 2 min. All potentials are given *versus* the Ag/AgCl electrode in saturated KCl solution

3. Results

The clean and well-annealed Ru(0001) surface is characterized by a well-defined (1 × 1)-structure without any impurities identified by AES. It is difficult to determine quantitatively the C-contamination on the Ru electrodes due to the overlap of Auger C- and Ru-signals at 272 eV. However, one can estimate the C-contamination by the Auger intensity ratio *I*_{272(Ru)}/*I*_{231(Ru)}. For a clean Ru surface the value of the Auger intensity ratio is *ca.* 1.8, a marked increase of this value indicates C-contamination on the Ru surfaces. The RHEED pattern reproduced in Fig. 1a exhibits continuous 2D-reflection rods characteristic of a smooth and flat Ru(0001) surface. The cleanliness of the surface (as a consequence of the impurity-free electrochemical cell) is also reflected by the data of cyclic voltammetry (CV) recorded with a sweep rate of 50 mV s^{–1} in 0.1 M HClO₄ solution as reproduced in Fig. 2a. Peaks at –0.1 V and +0.25 V signal the voltammetric features of H- and OH-adsorption, respectively, while the current density due to double layer charging between –0.05 V and +0.1 V is very low. The profile of the CV in Fig. 2a resembles the CV obtained from 0.1 M HClO₄ reported by Adzic *et al.*⁹

Prolonged argon ion bombardment in UHV at room temperature produces a strongly distorted ('rough') surface whose RHEED pattern exhibits pronounced intensity modulation

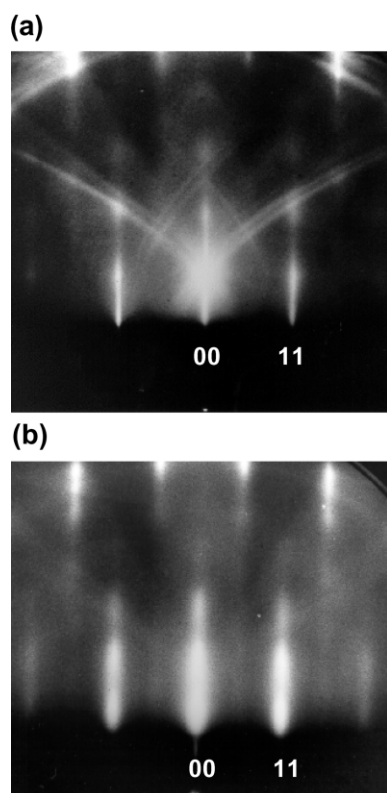


Fig. 1 Reflection high energy electron diffraction (RHEED) patterns from clean Ru(0001) surfaces. (a) Pattern along the [1120] azimuth from a smooth surface prepared by argon ion bombardment at 700 °C and subsequent annealing at 1000 °C in UHV. (b) Pattern along the [0110] azimuth from a rough surface prepared by prolonged argon ion bombardment at room temperature without subsequent annealing.

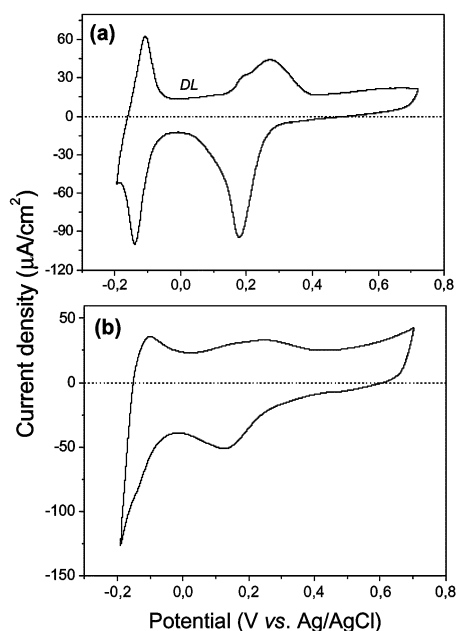


Fig. 2 Cyclic current–potential curves with scan rates of 50 mV s^{−1} in 0.1 M HClO₄ solution for Ru(0001) surfaces initially saturated by adsorbed CO. (a) Smooth surface, as with Fig. 1a. (b) Rough surface, as with Fig. 1b.

along the reciprocal lattice rods as shown in Fig. 1b. The resulting CV is reproduced in Fig. 2b and is quite different from that of the smooth surface. The pronounced redox couples for H- and OH-adsorption/desorption at −0.1 V and 0.25 V, respectively, are no longer discernible. This result is in line with previous findings, with Pt^{10–15} single crystal surfaces, whereafter distortion of the surface structure caused by redox cycles into the oxidation region is reflected by broadening of the peak profile for H-adsorption/desorption. In the present case it is suggested that the broad and structureless current distribution results from overlap of H- and OH-adsorption peaks originating from different facet planes and surface structural defects introduced by the sputtering process. These data are qualitatively similar to those reported for polycrystalline¹⁶ or only mechanically polished (0001) single crystal Ru electrodes,¹⁷ as well as for a Au(111) surface onto which 0.85 ML of Ru had been deposited and which exhibited numerous grain boundaries as identified by STM.¹⁸ On the other hand Lin *et al.*¹⁹ reported for a polished Ru(0001) electrode CV data with a sharp H-adsorption peak similar to our Fig. 2a for the smooth surface.

The electrosorption of CO_{ad} on the Ru(0001) electrode was performed by applying the optimum potential of −0.1 V for 2 min in a CO-saturated HClO₄ solution. The CV in CO saturated HClO₄ solution (see dotted line in Fig. 3a) for the CO-covered Ru(0001) electrode no longer shows H_{ad} and OH_{ad} peaks, due to complete blocking of adsorption of H and OH by CO_{ad} species, *i.e.*, the presence of a CO adlayer on Ru(0001) results in a strong reduction of the double-layer current density in the region between −0.2 V and +0.3 V. Subsequently, the CO-solution in the electrolyte vessel and the glass capillary were exchanged by a CO-free HClO₄ electrolyte by means of the flow-cell procedure under air-free atmospheric conditions.²⁰ The adsorbed CO was then oxidized during cyclic voltammetry with a scan rate of 50 mV s^{−1}. The positive potential limits of +0.9 V and +0.7 V were chosen so as to strip the pre-adsorbed CO from the flat Ru(0001) and rough Ru(0001) electrode surfaces, respectively, and in order to avoid irreversible disordering of the surface by place-exchange processes of OH and Ru. It should be noted that no significant

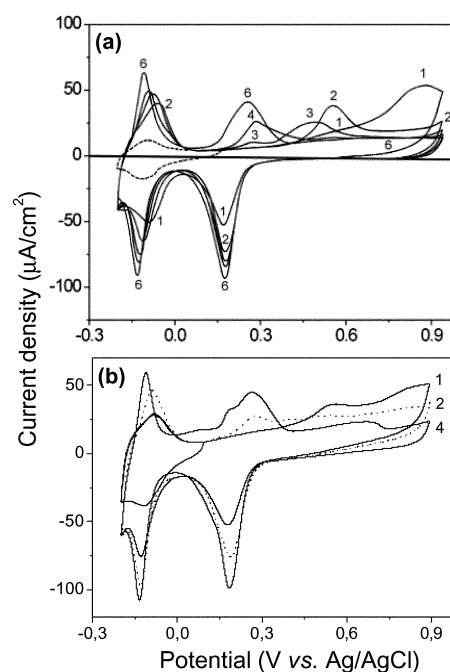


Fig. 3 Consecutive CV curves from a smooth Ru(0001) surface recorded with a scan rate of 50 mV s^{−1} in (CO free) 0.1 M HClO₄ solution. The sequence of scans is marked by numbers. (a) Surface initially saturated by CO (0.5 ML). (b) Initial CO coverage ~0.2 ML.

C-contamination was detected for the emersed Ru(0001) electrodes after electrochemical experiments as confirmed by the Auger intensity ratio $I_{272(\text{Ru})}/I_{231(\text{Ru})}$ of *ca.* 1.9 close to the value of a clean Ru surface.

The stripping voltammetry curve of saturated CO_{ad} (0.5 ML) on a flat Ru(0001) surface in 0.1 M HClO_4 is presented in Fig. 3a. There is no peak around +0.25 V, indicating that the formation of OH_{ad} is blocked by preadsorbed CO. The anodic current increases gradually at +0.4 V and a pronounced peak appears at +0.8 V on the first anodic scan, which is attributed to electrooxidation of CO_{ad} on Ru(0001), since there is no visible anodic peak at +0.8 V in the absence of adsorbed CO on Ru(0001) (as seen in Fig. 2a). On the second cycle, a new anodic peak appeared at a relatively low overpotential of +0.55 V where the oxidation of residual CO_{ad} by O-adspecies occurred, but the anodic peak at +0.8 V was almost absent. The concomitant adsorption of OH_{ad} is reflected by the reduction peak at +0.17 V on the first negative-going scan, which is clearly associated with the reduction of the O/ OH_{ad} species created during oxidative removal of CO_{ad} . On the third scan, the CO coverage had been reduced sufficiently so that the OH adsorption manifests itself as a small peak around +0.25 V; CO oxidation sets in shortly afterwards, with its peak maximum at +0.46 V. (A similar observation of CO-oxidation potential dependence on CO-coverage has also been made for CO electrooxidation on Pd(111).²¹) These findings indicate that CO oxidation requires coadsorbed oxygen species. For high CO coverage, oxygen adsorption can only be enforced at large overvoltage (first scan). At lower coverage, the oxidation sets in much earlier, the additional shift from +0.55 V to +0.46 V may be due to variations in binding energy for different $\text{O}_{\text{ad}}/\text{CO}_{\text{ad}}$ mixtures. The change of the CO_{ad} bonding state induced by oxidative removal of CO_{ad} is supported by *in-situ* IR measurements.²⁰ These show a coverage dependence of ν_{CO} for a CO-adlayer on the Ru electrode similar to the results observed for the change in ν_{CO} Pd(111) by partial electrooxidative removal of CO_{ad} .²¹ These results suggest that different bonding states of O/ CO_{ad} on the Ru(0001) surfaces due to different coverage ratios of O/CO do not co-exist on the Ru surface under steady-state conditions; *i.e.*, the bonding states of O/ CO_{ad} adlayers appearing in the second and third cycles are created as a result of oxidative removal of CO_{ad} *via* a relaxation process or a rearrangement of the CO_{ad} adlayer with the coadsorbed oxygenated species.

In order to investigate the dependence of the onset oxidation potential of CO on the coverage of CO on a smooth Ru(0001) surface, a lower coverage of CO on Ru(0001) was prepared by applying -0.1 V for 10 s in a CO-saturated HClO_4 solution. The resulting cyclic voltammetric profile of the Ru(0001) electrode with less CO_{ad} is shown in Fig. 3b. It is distinctly different from the cyclic voltammetry for a saturated CO coverage of 0.5 ML as reproduced in Fig. 3a. A pronounced CO-oxidation peak first occurred at a lower overpotential, +0.55 V, on the first cycle, the same potential as the second wave in Fig. 3a which occurred after partial removal of CO_{ad} by the first cycle. Thus the CO-oxidation potential is strongly coverage-dependent. It is worth mentioning that no discernible CO electrooxidation was found on Ru(0001) in 0.05 M H_2SO_4 solution as a result of CO desorption without oxidizing to CO_2 , whereas a pronounced oxidation peak developed on a Ru(1010) electrode surface in the same solution.²²

CO stripping voltammetry data for the rough Ru(0001) electrode is shown in Fig. 4: The electrooxidation of CO commences at +0.15 V and a pronounced broad peak appears around +0.35 V. Interestingly, it resembles the CV recorded for CO electrooxidation on a Au(111) electrode with deposited Ru in 0.1 M H_2SO_4 solution.¹⁸ Thus it is suggested that the sputtered Ru(0001) surface exhibits a similar surface morphology as this Ru-modified Au(111) surface. Complete oxidation

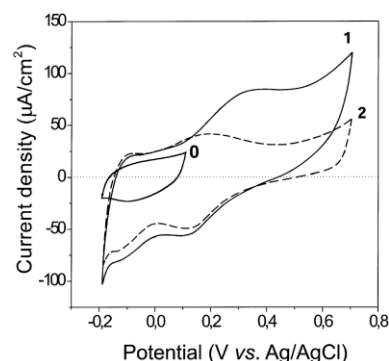


Fig. 4 CV curves from a rough Ru(0001) surface in 0.1 M HClO_4 recorded with 50 mV s^{-1} . Wave 0 denotes the CV after CO electrosorption before CO oxidative stripping. Waves 1 and 2 indicate the first and the second CO oxidative stripping, respectively.

of the CO monolayer on rough Ru(0001) was achieved by only one oxidative stripping scan, similarly as reported for the Ru-modified Au(111) surface.¹⁸ However, the results differ from those observed with the smooth Ru(0001) surface as shown in Fig. 3a, where the adsorbed CO was completely removed only after more than three oxidative stripping cycles.

Note that in a CO-free electrolyte OH formation has already reached its peak at +0.19 V. The oxidation of preadsorbed CO sets in at about the same voltage. Thus there is no significant inhibition of adsorption of oxygen species on a rough surface, even when saturated with CO_{ad} .

In order to obtain additional information on the chemical composition of the Ru electrode surface *ex-situ* AES measurements were performed for the Ru electrodes emersed at various electrode potentials. The Auger O/Ru intensity ratio ($I_{\text{O}}/I_{\text{Ru}}$) for the rough Ru(0001) electrode emersed at +0.3 V is approximately three times higher than that obtained from a smooth Ru electrode. This suggests that an oxygen adlayer is already formed at +0.3 V on the rough Ru surface, corresponding in coverage to the O-adlayer formed at +0.7 V on the smooth Ru electrode surface. Furthermore, diffuse (1×1) patterns with increased background intensity observed by LEED/RHEED suggested the formation of an amorphous oxide layer on the rough Ru(0001) surface, in agreement with reports on STM images for the Ru deposited Au(111) surface in the same potential range.¹⁸ This oxide-layer on a rough Ru surface differs from the (100) RuO_2 -oxide formed on a flat Ru(0001) surface at $E > +1.0$ V where the crystalline oxide was formed with concomitant Ru dissolution as evidenced by RHEED.²³ The higher oxygen concentration on a rough Ru(0001) surface obviously decreases the overpotential for CO oxidation.

Not surprisingly the current–time transients of CO oxidation on a smooth Ru(0001) surface when stepping to a constant potential depend strongly on the applied overpotential.²⁴ For comparison of the oxidation rate of CO_{ad} on a rough Ru(0001) surface with that on a smooth Ru surface, the current responses at four different oxidation potentials were measured on a rough Ru electrode. Fig. 5a shows current–time transients for the oxidation of adsorbed CO on a rough surface at a potential of +0.4 V. For reference, the dotted current–time curve, in 0.1 M HClO_4 prior to electro-sorption of CO on rough Ru(0001) represents the double layer charging and oxidation charging current. After a sharp increase, the transient (solid line) in Fig. 5a decays for several seconds and then reaches the steady state current value. After subtracting the double layer current, the charge for mere CO oxidation results as $259 \mu\text{C cm}^{-2}$ which corresponds to *ca.* 0.5 ML of CO oxidation on a flat Ru(0001) surface.¹⁹ From comparison of CO oxidation on a smooth Ru(0001) surface

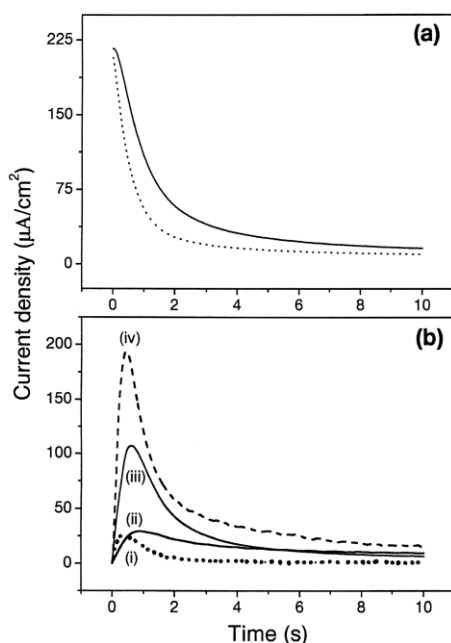


Fig. 5 Current transients from a rough, CO saturated Ru(0001) surface in 0.1 M HClO₄. (a) Potential step from -0.1 V to $+0.4$ V (vs. Ag/AgCl). The double layer oxidation charging in CO-free solution is indicated by the dotted line. (b) Current density after subtraction of the double layer and oxidation charging for steps to various potentials: (i) = $+0.17$ V, (ii) = $+0.26$ V, (iii) = $+0.4$ V, and (iv) = $+0.6$ V.

with a saturated CO-coverage of 0.5 ML^{24} with this higher oxidation rate of CO at $+0.4$ V, a roughness factor of two can be estimated.

In Fig. 5b, the CO oxidation charge at $+0.17$ V for a reaction duration of 10 s is $43 \mu\text{C cm}^{-2}$, which indicates that 0.084 ML of CO can be oxidized. This charge for CO oxidation significantly increases at higher oxidation overpotential. A high oxidation charge of $446 \mu\text{C cm}^{-2}$ is obtained at $+0.6$ V and it is attributed to *ca.* 0.87 ML adsorbed CO on the rough Ru electrode. On the other hand, there were no detectable current–time transients for CO oxidation even at $+0.55$ V on flat Ru(0001). These characteristics are consistent with responses that have been observed in cyclic voltammetry measurements involving CO oxidation. Note that the kinetics of CO oxidation on a Ru(0001) surface depends on facets, defects, and steps generated by Ar⁺ sputtering.

Table 1 summarises the charge of the current transients for CO oxidation on rough and smooth Ru(0001) electrodes whereby the following interesting fact was noted: On a rough Ru(0001) surface, a finite charge for CO oxidation even at a very low overpotential ($+0.17$ V), is observed, unlike with the smooth Ru(0001) surface. As already mentioned above, we obtain *ca.* 0.5 ML oxidation current at $+0.4$ V on a rough Ru(0001) electrode and this value can be only achieved at $+0.95$ V on a smooth Ru surface. At $E_{\text{app}} \geq +0.65$ V, rough

Ru can be oxidized, at about $+0.8$ V oxygen evolution started. Summarizing these experimental data, a rough Ru surface can significantly decrease the overpotential for CO tolerance in a hydrogen fuel cell.

4. Discussion

The CV data for the smooth Ru(0001) electrode demonstrate that the current density is markedly reduced in the double-layer region after adsorption of CO, indicating that the presence of this species inhibits charge transfer across the interface. Up to $+0.5$ V, no current peak appeared in the stripping voltammetry from a CO + O/OH precovered Ru(0001) surface, in accordance with previous current transient measurements,²⁴ and a pronounced peak only showed up at $+0.85$ eV. This behavior is also reflected by the findings for a Ru(0001) surface in contact with gaseous CO and/or O₂: In contrast to Pt(111), CO and O coadsorbed on Ru(0001) do not react to give CO₂ because of the too strong Ru–O bond. With increasing O coverage the binding energy of this species decreases markedly until the monolayer is completed with a (1×1) -structure,²⁵ but at the same time also bonding of CO becomes weaker and is eventually completely inhibited at room temperature.²⁶ Only transformation into a thin RuO₂ overlayer exposing its (110) plane by severe oxygen exposures creates a surface which is catalytically highly active,²⁷ but this stage can be reached by anodic oxidation only if the potential is increased to ≥ 1.1 V,²⁸ which was consequently avoided in the present study.

On the other hand, CO preadsorbed on either Pt(111) or Ru(0001) beyond a critical coverage inhibits chemisorption of oxygen from the gas phase which hence requires an increase of the temperature for thermal desorption of CO. In this respect the situation is obviously somewhat different under electrochemical reaction conditions: Anodic polarization weakens both the Ru–CO and Ru–O bond, so that on the one hand O- (resp. OH-) formation becomes possible even with a CO-covered surface and on the other the Ru–O bond becomes sufficiently weakened to enable CO₂ formation. The latter process requires with the smooth Ru(0001) surface an overpotential of about 0.85 V.

However, there exists a complex interplay between the energetics and the surface concentrations of the species involved. The varying CO-electrooxidation potentials observed during different CV cycles are attributed to the change in CO coverage. In Fig. 3a the lower CO-oxidation potential ($+0.55$ V) on the second cycle results presumably from reaction from a stage with reduced CO coverage. This is confirmed by an additional CO stripping experiment (Fig. 3b) with a lower concentration of CO_{ad} (about 0.2 ML). This coverage is comparable to that remaining on the surface underlying Fig. 3a after the first CV cycle, and accordingly the CO-oxidation potential ($+0.55$ V) is very similar in both cases.

The oxidative removal of part of the CO during the first cycle results in additional uptake of oxygen, as demonstrated

Table 1 The CO oxidation charge evaluated from the current vs. time transients (chronoamperometry) for the smooth¹⁸ and rough Ru(0001) electrode stepped to various potentials

Overpotential (E_{app})	Electrocatalytic oxidation charge of CO, $Q_{\text{CO}}/\mu\text{C cm}^{-2}$	
	Rough Ru(0001)	Flat Ru(0001)
$+0.17$ V	43	–
$+0.26$ V	150	–
$+0.40$ V	259	–
$+0.60$ V	446	83
$+0.75$ V	Ru oxide	161
$+0.95$ V	Ru oxide or O ₂ ↑	226

by the reduction peak at +0.17 V in the reverse scan direction. This change of the surface composition (*i.e.* O/CO ratio) causes also lowering of the adsorption energies of both species,^{26,29} and hence the CO-oxidation in the next cycle occurs at lower potential. Partial removal of CO accompanied by O adsorption has also been found with *in-situ* IR measurements.³⁰ These experiments also revealed a shift of the C–O stretch frequency from 2010 cm^{−1} at 0.0 V to 2040 cm^{−1} at 0.8 V, reflecting a weakening of the Ru–CO bond through reduction of the electronic ‘back-bonding’ contribution. A similar effect, on the other hand, had also been reported with UHV measurements if O was coadsorbed with CO.³¹ Interestingly, the ease of CO_{ad} electrooxidation has also been observed to increase at lower CO coverage formed from formic acid or CO electrosorption on Pt-group metals^{32,33} which is attributed to the presence of adjacent sites for the adsorption of the electrochemical oxidant, resembling the behavior of CO electrooxidation on Ru(0001).

The rough Ru(0001) surface was found to exhibit a much higher electrocatalytic activity than the smooth sample: CO oxidation commences already at +0.15 V and a pronounced broad peak is centered at +0.35 V, *i.e.* in a potential range where the smooth Ru(0001) electrode shows no appreciable activity at all. This activity is comparable to that of a porous Pt electrode where CO-oxidation occurs also at a less positive potential (0.35 V) compared to a flat Pt(111) surface (0.55 V),^{25,34,35} albeit that with the rough Ru(0001) surface the CO stripping peak is broader, presumably because of contributions from various structure elements (facets *etc.*) of the surface. Moreover, almost complete oxidation occurs during the first cycle, again similarly as with Pt(111)^{31,32} or a Ru-modified Pt(111) surface.²⁰ The higher activity of the rough Ru(001) surface has to be sought in its ability for the uptake of larger concentrations of oxygen by the high density of surface defects and high-index facets, leading even to the formation of an amorphous ‘oxide-like’ phase presumably similar to RuO₂. The associated weaker Ru–O bond then also enables higher reactivity. In addition, with the rough surface the Ru atoms exhibit enhanced mobility. This had been demonstrated by means of RHEED where the pattern showed sharpening of the reflection rods after CO electrooxidation, *i.e.* smoothening of the Ru substrate in the course of the reaction.

The behavior of the rough Ru(0001) surface, which may correspond to Ru nano-particles attached to the Ru(0001) surface, exhibits similarities to the properties of small Ru particles being present with bimetallic Pt/Ru electrocatalysts,^{3,36} where the activity is obviously again governed by surface defects and higher index facets like Ru(1010).²²

References

- 1 A. Hamnett, *Interfacial Electrochemistry: Theory, Experiment and Applications*, ed. A. Wieckowski, Marcel Dekker Inc., New York, 1999, p. 843.
- 2 H. A. Gasteiger, N. Markovic, P. N. Ross and E. J. Cairns, *J. Phys. Chem.*, 1993, **97**, 12020.
- 3 W. Chrzanowski and A. Wieckowski, *Langmuir*, 1998, **14**, 1967.
- 4 M. Krausa and W. Vielstich, *J. Electroanal. Chem.*, 1994, **379**, 307.
- 5 M. Watanabe and S. Motoo, *J. Electroanal. Chem.*, 1975, **60**, 267.
- 6 E. Ticanelli, J. G. Beery, M. T. Peffett and S. Gottesfeld, *J. Electroanal. Chem.*, 1989, **258**, 61.
- 7 G. Lehmppfuhl, Y. Uchida, M. S. Zei and D. M. Kolb, in *Imaging of Surfaces and Interfaces: Frontiers of Electrochemistry*, ed. J. Lipkowsky and P. N. Ross, Wiley-VCH, Weinheim, 1999, vol. 5, p. 57.
- 8 W. F. Lin, M. S. Zei, Y. D. Kim, H. Over and G. Ertl, *J. Phys. Chem. B*, 2000, **104**, 6040.
- 9 J. X. Wang, N. S. Marinkovic, H. Zajonz, B. M. Ocko and R. R. Adzic, *J. Phys. Chem. B*, 2001, **105**, 2809.
- 10 F. Wagner and P. F. Ross, *Surf. Sci.*, 1985, **160**, 305.
- 11 K. Wu and M. S. Zei, *Surf. Sci.*, 1998, **415**, 212.
- 12 R. Ishikawa and A. Hubbard, *J. Electroanal. Chem.*, 1976, **69**, 317.
- 13 K. Itaya, S. Sugawara, K. Sashikata and N. Furuya, *J. Vac. Sci. Technol. A*, 1990, **8**.
- 14 D. Aberdam, R. Durand, R. Faure and F. El-Omar, *Surf. Sci.*, 1986, **171**, 303.
- 15 H. Angerstein-Kozłowska, B. Conway and W. Sharp, *J. Electroanal. Chem.*, 1973, **43**, 9.
- 16 S. Hadzi-Jordanov, H. Angerstein-Kozłowska, M. Vukovic and B. E. Conway, *J. Electrochem. Soc.*, 1978, **125**, 147.
- 17 P. C. Lu, C. H. Yang, S. L. Yau and M. S. Zei, *Langmuir*, submitted.
- 18 S. Strbac, F. Maroun, O. M. Magnussen and R. J. Behm, *J. Electroanal. Chem.*, 2001, **500**, 479.
- 19 W. F. Lin, P. A. Christensen and A. Hamnett, *J. Phys. Chem. B*, 2000, **104**, 12002.
- 20 W. F. Lin, M. S. Zei, M. Eiswirth, G. Ertl, T. Iwasita and W. Vielstich, *J. Phys. Chem. B*, 1999, **103**, 6968.
- 21 Z. Zou, R. Gomez and M. J. Weaver, *J. Electroanal. Chem.*, 1999, **474**, 155.
- 22 S. R. Brankovic, J. X. Wang and R. R. Adzic, *The 53rd Meeting of ISE*, San Francisco, CA, 2001, Abstract No. 1049.
- 23 M. S. Zei and G. Ertl, *Phys. Chem. Chem. Phys.*, 2000, **2**, 3855.
- 24 W. B. Wang, M. S. Zei and G. Ertl, *Phys. Chem. Chem. Phys.*, 2001, **3**, 3307.
- 25 C. Stampfl, S. Schwegmann, H. Over, M. Scheffler and G. Ertl, *Phys. Rev. Lett.*, 1996, **77**, 3371.
- 26 F. M. Hoffmann, M. D. Weisel and C. H. F. Peden, *Surf. Sci.*, 1991, **253**, 59.
- 27 H. Over, Y. D. Kim, A. P. Seitsonen, S. Wendt, E. Lundgren, M. Schmid, P. Varga, A. Morgante and G. Ertl, *Science*, 2000, **287**, 1474.
- 28 Y. D. Kim, A. P. Seitsonen, S. Wendt, J. Wang, C. Fan, K. Jacobi, H. Over and G. Ertl, *J. Phys. Chem. B*, 2001, **105**, 3752.
- 29 C. H. F. Peden, D. W. Goodman, M. D. Weisel and F. M. Hoffmann, *Surf. Sci.*, 1991, **253**, 44.
- 30 W. F. Lin, P. A. Christensen, A. Hamnett, M. S. Zei and G. Ertl, *J. Phys. Chem. B*, 2000, **104**, 6642.
- 31 F. M. Hoffmann, *Surf. Sci. Rep.*, 1983, **3**, 107.
- 32 N. M. Markovic, B. N. Grgur, C. A. Lucas and P. N. Ross, *J. Phys. Chem. B*, 1999, **103**, 487.
- 33 M. F. Mrozek, H. Luo and M. J. Weaver, *Langmuir*, 2000, **16**, 8463.
- 34 R. Ianniello, V. M. Schmidt, U. Stimming, J. Stumper and A. Wallau, *Electrochem. Acta*, 1994, **11**, 1863.
- 35 A. Wieckowski, M. Rubel and C. Gutierrez, *J. Electroanal. Chem.*, 1995, **382**, 97.
- 36 E. Herrero-Rodriguez, J. M. Felin and A. Wieckowski, *Langmuir*, 1999, **15**, 4944.